Instantaneous mapping of high-latitude convection with coherent HF radars

C. Hanuise, C. Senior, J.C. Cerisier, Jean-Pierre J Villain, R.A. Greenwald, J.M. Ruohoniemi, K. B. Baker

JOURNAL OF GEOPHYSICAL RESEARCH, VOL. 98, NO. A10, PAGES 17,387–17,400, OCTOBER 1, 1993

Instantaneous Mapping of High-Latitude Convection With Coherent HF Radars

C. HANUISE,[1] C. SENIOR,[2] J.-C. CERISIER,[2,3] J.-P. VILLAIN,[4] R. A. GREENWALD,[5] J. M. RUOHONIEMI,[5] AND K. B. BAKER[5]

Coherent HF radars at Goose Bay (Labrador) and Schefferville (Quebec) are used to study plasma convection in the high-latitude ionosphere. Maps of the two-dimensional flow pattern are obtained by merging simultaneous sets of radial velocity data, each with a time resolution of a few minutes. From a time sequence of such maps we have separated the changes in flow due to magnetic local time (MLT) variations over the region of observation, from those due to UT time variations. We study in detail the convection in the early morning sector observed on October 15, 1989, when the interplanetary magnetic field (IMF) reversed from southward to northward. This IMF reversal was not associated with a clear response in the nightside convection but rather with several sudden changes, some of which anticipated the B_z reversal. We suggest that these changes are associated with delayed and superposed ionospheric responses to previous IMF perturbations, or to local effects. After the IMF reversal from south to north our observations of westward and southwestward velocities in the 71°-77° invariant latitude range are consistent with the earlier simulations for $B_z > 0$ and $B_y < 0$. During the period of steady northward IMF after the reversal the convection pattern was observed to reconfigure slowly: a region of large westward velocities progressively moved poleward, while convection in the low-latitude part of the field of view faded away. The time constant of this slow reconfiguration was about 1 hour and varied with MLT, such that it was larger closer to midnight. These data, combined with particle data from successive passes of the DMSP satellites, provide information on the contraction of the polar cap after the IMF B_z reversal and on the MLT dependency of the velocity at which this contraction occurs. They show that the polar cap contracts more rapidly in the daytime than in the nightime and more rapidly in the postmidnight sector than in the premidnight sector.

INTRODUCTION

Plasma convection in the magnetosphere is a highly dynamic process, driven by fluctuations of interplanetary medium parameters close to the magnetopause. The orientation of the interplanetary magnetic field (IMF) is known to be a very important factor in controlling convection, through reconnection processes at the magnetopause between the Earth and the interplanetary fields. Experimental methods for observing convective flow patterns are based either on low-altitude polar-orbiting satellites, which provide nearly instantaneous latitudinal cuts through the high-latitude region, or on radars that provide convection maps by means of beam-scanning techniques and by using the drift of the radar in magnetic local time (MLT). During the last decade, HF coherent radars have demonstrated their unique capability in measuring convection velocity over large areas with a high time resolution [*Hanuise et al.*, 1981; *Greenwald et al.*, 1985]. At high latitudes, where the Earth's magnetic field is close to vertical, refraction of the HF radar wave causes the wave vector to become perpendicular to the Earth's magnetic field, leading to an enhanced backscattering cross section. At F region altitudes the irregularities at decametric wavelengths have been shown to be stationary in the plasma frame and thus their Doppler velocity can be safely identified with the radial component of the plasma convection velocity [*Villain et al.*, 1985; *Ruohoniemi et al.*, 1987].

The Johns Hopkins University Applied Physics Laboratory HF radar located at Goose Bay, Labrador, has been operational since 1983. However, a monostatic radar can only measure the radial component of the velocity of irregularities embedded in the plasma. In order to obtain a full vector determination a second radar facility covering the same field of view was later built in Schefferville, Quebec, by French groups led by the University of Toulon, becoming fully operational in October 1989. In the meantime a method had been developed to derive vector velocity maps from a single radar [*Hanuise et al.*, 1985; *Ruohoniemi et al.*, 1988, 1989]. It relies, however, on the additional assumption of longitudinal uniformity of the plasma flow, which is only valid for a class of simple convection patterns [see *Freeman et al.*, 1991]. When only a limited subset of vector velocities can be determined from dual radar data, it is possible to extend the map to regions where data from only one radar are available, assuming that the flow is divergence free. This has proven to be particularly useful when one of the radars is operated in a single-beam mode, as was the case for the Schefferville radar before October 1989 [*Ruohoniemi et al.*, 1989]. The zero divergence assumption has also been used to modify the initial vector velocity map deduced from the longitudinal uniformity hypothesis.

The HF multibeam radars have already shown their ability at describing convection changes with a high temporal resolution. Results from the Goose Bay radar and its sister radar at Halley Bay, Antarctica, that covers the magnetically conjugate area, showed the rapid reconfiguration of the convection pattern in the noon sector following IMF changes. For example, *Greenwald et al.* [1990] showed that the convection response in the noon sector to a change in the B_y component of the IMF is about 8 min.

In this paper we develop a method for deriving vector velocity maps by merging radial velocities from the two radars, with no additional assumption. From a time series of such maps we can then separate, in the changes which occur

[1]Laboratoire de Sondages Electromagnétiques de l'Environnement Terrestre / CNRS, Université de Toulon et du Var, La Garde, France.

[2]Centre de Recherches en Physique de l'Environnement / CNRS, Saint-Maur-des-Fossés, France.

[3]Also at Université Pierre et Marie Curie, Paris, France.

[4]Laboratoire de Physique et Chimie de l'Environnement / CNRS, Orléans, France.

[5]Applied Physics Laboratory, Laurel, Maryland.

Paper number 93JA00813.
0148-0227/93/93JA-00813$05.00

from map to map, those which are due to the drift in MLT of the common field of view of the two radars, from the "true" time variations as they should be observed in a solar magnetospheric frame. We thus obtain, as did *Shen and Nielsen* [1987] from the VHF Scandinavian Twin Auroral Radar Experiment (STARE) and Sweden and Britain Radar Experiment (SABRE) radars, the time evolution of latitudinal profiles of the convection velocity at a fixed MLT. We illustrate these methods with an example showing the modification of the convection pattern in the early morning sector after a northward turning of the IMF B_z component.

DESCRIPTION OF THE HF RADARS

The data presented in this paper were acquired with a pair of two HF radars located in northeastern Canada. The radar operated from Goose Bay, Labrador (53.3°N, 60.5°W), has been described in detail by *Greenwald et al.* [1983]. The second radar facility, named Sherpa (Système HF d'Etudes Radar Polaires et Aurorales), is located in Schefferville, Quebec (54.8°N, 66.8°W), and has basically similar characteristics. Both detect waves backscattered from ionospheric irregularities over northeastern Canada and Greenland, at invariant latitudes higher than 65°.

The respective fields of view are determined by the antenna arrays, which are used for both transmitting and receiving. In Goose Bay the main array comprises 16 log periodic antennas operating between 8 and 20 MHz. The azimuthal resolution is 3° to 5°, depending upon frequency, and the beam can be oriented in 16 directions ranging from 20° west to 30° east of geographic north, with an azimuthal scan step of 3.3°. In Schefferville the array comprises only eight log periodic antennas identical to those in Goose Bay. The azimuthal resolution is consequently decreased by a factor of 2. The normal to the array is directed 15° east of geographic north. The beam can also be electronically switched over an azimuth of 50°, from 10° west to 40° east of geographic north. In a given direction the backscattered signal is usually sampled for fifty 45-km-wide range gates, the near and far radar horizons for sampling being set at 300 and 2550 km. Thus each radar potentially monitors the irregularity activity over nearly 1.4 million km^2 of the high-latitude ionosphere. Most of this area is common to both instruments (Figure 1).

The data were obtained while the two radars were in their usual operating modes. In Goose Bay a scan sequentially samples the 16 beams, starting from the westernmost direction. The integration time is typically set to 5 s for each beam position, thus completing a sequence in 80 s. The radar transmits on a fixed frequency, which is changed during the day to adapt to the propagation conditions prevailing at different local times. At Schefferville, due to the wider beamwidth each scan samples only the eight even beams out of the 16 possible beam directions. To complete a sequence with the same time resolution, the integration time is increased to 10 s. Moreover, two radar frequencies are systematically used (11 MHz and 14 MHz) which reduces the time resolution for a given frequency but has the advantage of extending the geographic coverage, owing to changes in wave propagation with variation of the sounding frequency.

For each beam/range radar cell, a 17-lag complex autocorrelation function is computed in real time [*Greenwald et al.*, 1983]. During the observations reported here those associated with scatter are recorded on magnetic tape and, subsequently, are processed to obtain estimates of signal-to-noise ratio, mean Doppler velocity, correlation time, and root-mean-square error estimates [*Villain et al.*, 1987]. Information on the irregularity characteristics and, in particular, the Doppler velocity is thus available over a large part of the radar fields of view.

DERIVATION OF VELOCITY MAPS

Since modern HF radars started observations, doubts have been expressed on their ability to map ionospheric convective motions. First, the question of whether plasma motion can be derived from Doppler velocity was resolved, at least for F region irregularities, by several experimental comparisons between HF and incoherent scatter radars [*Villain et al.*, 1985; *Ruohoniemi et al.*, 1987]. These comparisons confirmed theoretical expectations [*Keskinen and Ossakow*, 1983] that the Doppler velocity of such irregularities is equal to the plasma drift velocity. The second doubt concerned the capability of HF radars to locate scattering sources with enough precision. Usually, the electron density distribution necessary to determine the HF propagation conditions and thus to determine precisely the scattering region is not available. The situation becomes even more complex because of the variable nature of ionospheric density structures at high latitudes. Fortunately, ray-tracing studies using representative density profiles [*Villain et al.*, 1984] have shown that for typical ionospheric conditions the actual distance to a scattering region will generally be 15-30 km less than that predicted using a free space propagation hypothesis [*Baker et al.*, 1986], i.e., less than the size of a radar resolution cell. Consequently, if one accepts this limitation on spatial resolution, HF radars are suitable for studying ionospheric plasma motions. This is particularly true for mapping large-scale convective patterns.

The two-dimensional plasma drift velocity in a plane perpendicular to the Earth's magnetic field is derived by combining Doppler velocity data from the two radars. Figure 2

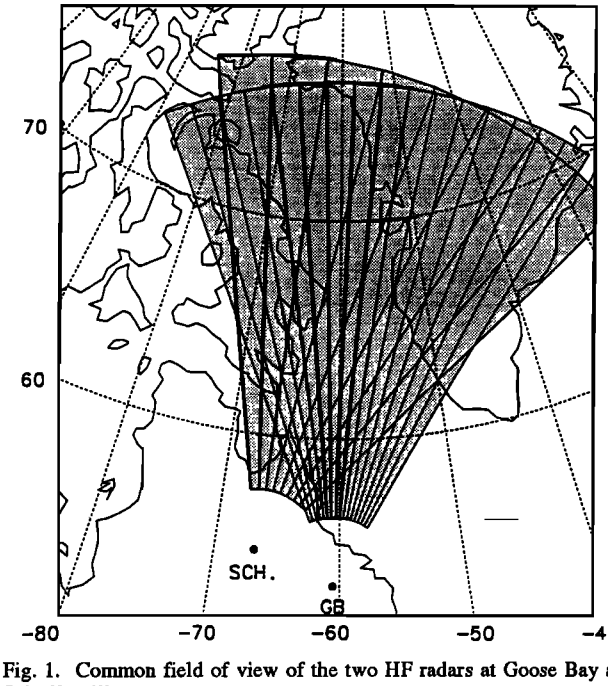

Fig. 1. Common field of view of the two HF radars at Goose Bay and Schefferville.

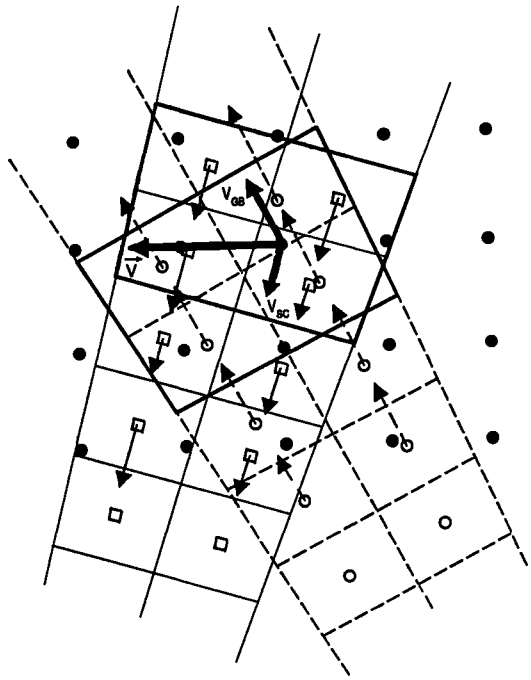

Fig. 2. Illustration of the method used for merging the data sets of radial velocities, provided by the two radars during the same time interval, into a single-vector velocity map. The solid circles represent the geographic grid points, while the open squares and circles, respectively, are the Schefferville and Goose Bay data points.

summarizes the method for deriving velocity vectors from the two radial components. Estimates of the radial velocity are obtained in each resolution cell, whose size is 45 km in the radial direction and 3°-5° in azimuth. At ranges where scattering is most commonly detected, a resolution cell roughly is a rectangle of 45 by 60 km. For the Schefferville data, odd beam directions are filled in by interpolating velocities measured on the two nearest even beams, so that the spatial resolution is formally identical for the two radars.

Vector velocities are computed at each point of a geographic grid, with a mesh size of half a degree in latitude and 1° in longitude. Spacing between grid points is therefore approximately 50 km along each axis over the radar field of view. At each grid point, the four nearest possible data points are determined for each radar. This is achieved by computing the azimuth of the grid point and its distance to the radar and by looking for data points on bracketing beams and ranges. In the following step, a mean radial velocity at the grid point is computed for each radar, with a weighting function proportional to the inverse distance between the grid point and the data point. Data points located at more than 100 km from the grid point are excluded. Finally, both mean radial velocities are geometrically combined to derive the two-dimensional vector velocity.

A velocity is derived only when at least two of the four possible valid data points are present for each radar. Several checks eliminate invalid or doubtful data: the signal-to-noise ratio must be larger than 3 dB; data quality checks eliminate bad data points; echoes identified as ground scatter are also eliminated; finally, the root-mean-square error on the velocity estimate must be less than 50 m/s. This might seem to be a low value, but experience shows that the error remains below 20 m/s in most cases. Large values are generally due to the presence of multipeaked Doppler spectra in the radar cell, which have to be eliminated for velocity computations. If necessary, error bars on magnitude and azimuth of the velocity vectors can be calculated. They depend on data quality and on the angle between the lines of sight of the two radars. This angle varies over the field of view from 45° at short ranges to less than 20° farther out, and it generally decreases from the center toward the edge of the field of view. Velocity estimates therefore will have a large uncertainty in regions of the common field of view where the angle between the two radar lines of sight is small.

At this stage of the processing, the velocity field is obtained in a geographic coordinate system, which can be transformed into either a geomagnetic or an invariant latitude/MLT coordinate system. The transformation uses a variation of the corrected geomagnetic coordinate system, as defined by *Baker and Wing* [1989]; based on the IGRF 85 magnetic field model updated to 1989, it provides analytical expressions relating geographic coordinates to magnetic coordinates at any altitude. The relation is smooth over the entire globe, even near the poles. Moreover, in order to derive magnetic local time at a given geographic position for a given UT, the transformation takes into account the effects of seasonal variations in the Sun's declination, along with the variation in the Sun's apparent position due to the eccentricity of the Earth's orbit. For a fixed point and a fixed UT these effects result in a MLT variation which reaches ± 20 min over the course of a year.

An example of the result of this radial velocity merging process is given in Figure 3, in a geomagnetic frame of reference. Figures 3*a* and 3*b* show the Doppler velocities observed at Goose Bay and Schefferville, respectively, on October 15, 1989 for the period 0557 UT to 0600 UT. These maps were obtained by averaging data from successive scans over a 3-min period. The velocity scale is given in the top left corner of the figure. Each velocity is represented by a straight line, the length of which represents the magnitude of the velocity. In Goose Bay, scatter is detected at invariant latitudes ranging from 68° up to 78° on the 16 beams. Radial velocities are directed toward the radar on most beams. Large radial velocities, up to 500-600 m/s, are measured in the northern part of the central beams, while low velocities are present on both edges and in the southern part of the map. These features indicate that the flow is not uniform over the field of view. The Schefferville data (Figure 3*b*) were observed over a slightly smaller region but in the same latitude range. Radial velocities are directed toward the radar, with magnitudes of 500-700 m/s for the high-latitude part of most beams except the easternmost one.

The vector velocity map resulting from the combination of Goose Bay and Schefferville observations is shown as Figure 3*c*. The dots represent the position of the grid point where the velocity is determined, the length of the straight lines is the magnitude of the vector velocity, and their direction is the plasma-flow line in the chosen coordinate system. This means that projections of a vector cannot be interpreted as the longitudinal and latitudinal components of velocity, except where the spatial scales of the axes are commensurate. The map covers the region of observation common to both radars. The flow direction is westward everywhere, with a marked southward component in the northwestern part of the map and a northward component in the eastern part of the map. As expected from the radial velocity maps, the flow is slow in the

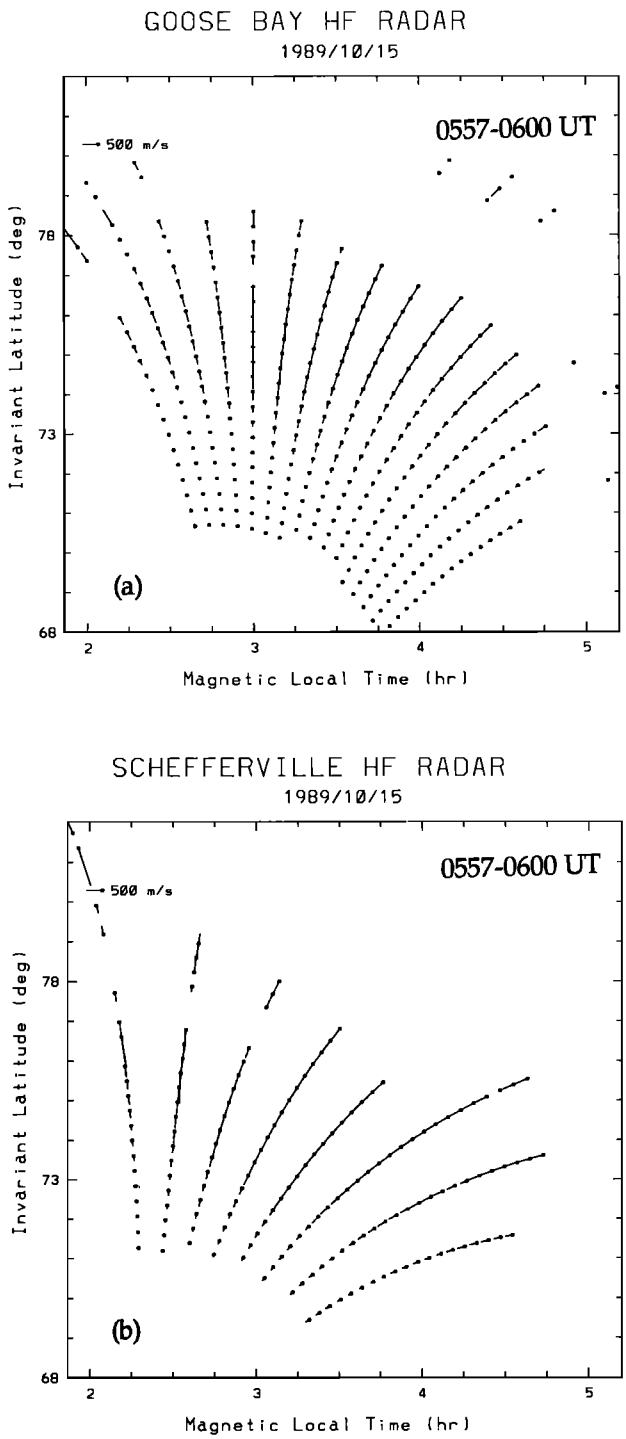

Fig. 3. Example of velocity maps obtained between 0557 and 0600 UT, in a geomagnetic frame of reference. (*a*) Radial velocity map for the Schefferville radar. (*b*) Radial velocity map for the Goose Bay radar.

south. We do not intend to discuss in this section the physical interpretation of this map, but we can note that it covers a sector of more than 2 hours in MLT for a given UT. A sequence of such maps therefore offers an excellent opportunity to study variations of the convection pattern as a function of UT for a fixed MLT and during about 2 hours of UT time. This will help to separate spatial and temporal variations in the plasma convection, the result of which will be presented hereafter.

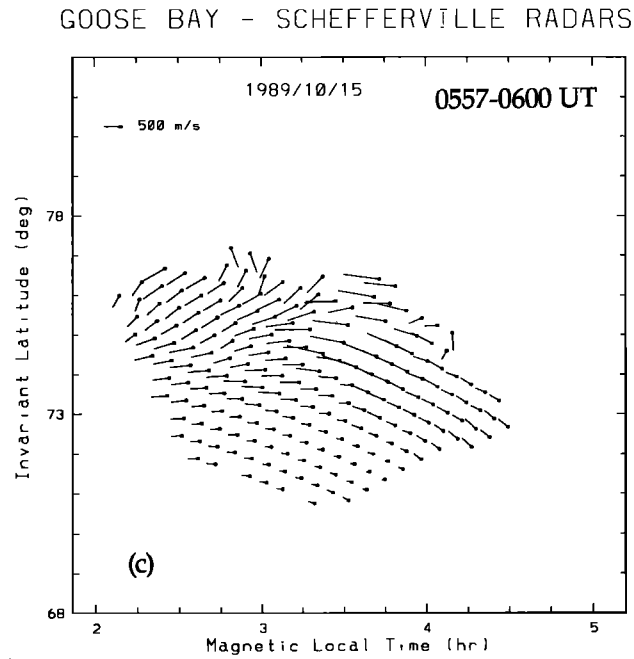

Fig. 3. (*c*) Vector velocity map obtained by merging the two maps of Figures 3*a* and 3*b*.

EXPERIMENTAL RESULTS

Geophysical Conditions

The results presented in this paper are focused on the nighttime, early morning hours of October 15, 1989. Interplanetary magnetic field (IMF) data from IMP8 were available for that period, and 30-s averages are plotted in Figure 4, in a GSM coordinate system. Also indicated in the top three panels is the GSM location of the satellite (in units of Earth radii) at the time shown by the arrows. The satellite was located above the magnetic equatorial plane upstream of the Earth, in the dawn sector at about 30 R_e and was traveling sunward. Figure 4 shows that the magnitude of the field decreases abruptly from 12-13 nT to about 10 nT at 0455 UT, which indicates that the satellite may have crossed the bow shock at that time, going from the magnetosheath to the interplanetary medium at X≈8.2 R_e and Y≈-30 R_e, i.e., at a very large distance from the Earth. One-hour averages of the IMP8 plasma data recorded after 0800 UT indeed indicate that the solar wind pressure was low on that day, with densities of ≈5 cm^{-3} and velocities of ≈350 $km.s^{-1}$. At 0433 UT the IMF B_z component reversed from southward to northward and remained positive afterward, varying between +2 nT and +7 nT, with a short uncertain period due to a data gap between 0438 UT and 0452 UT. The B_y component remained negative during the whole period, decreasing from a level of -11 nT to about -4 nT at the presumed time of the bow shock crossing.

The level of magnetic activity was very low during the 3-day period preceding the observations from October 13 to 15, these days being the three quietest days of the month. The maximum value of the Kn index was 1⁻ over the 48 hours before the northward turning of the IMF and 1 during the 3-hour period that includes this reversal. The magnetograms from the Greenland and Canopus (central Canada) magnetometer chains were extremely quiet between 0200 UT and 0800 UT. For both chains the largest fluctuations in the north-south horizontal

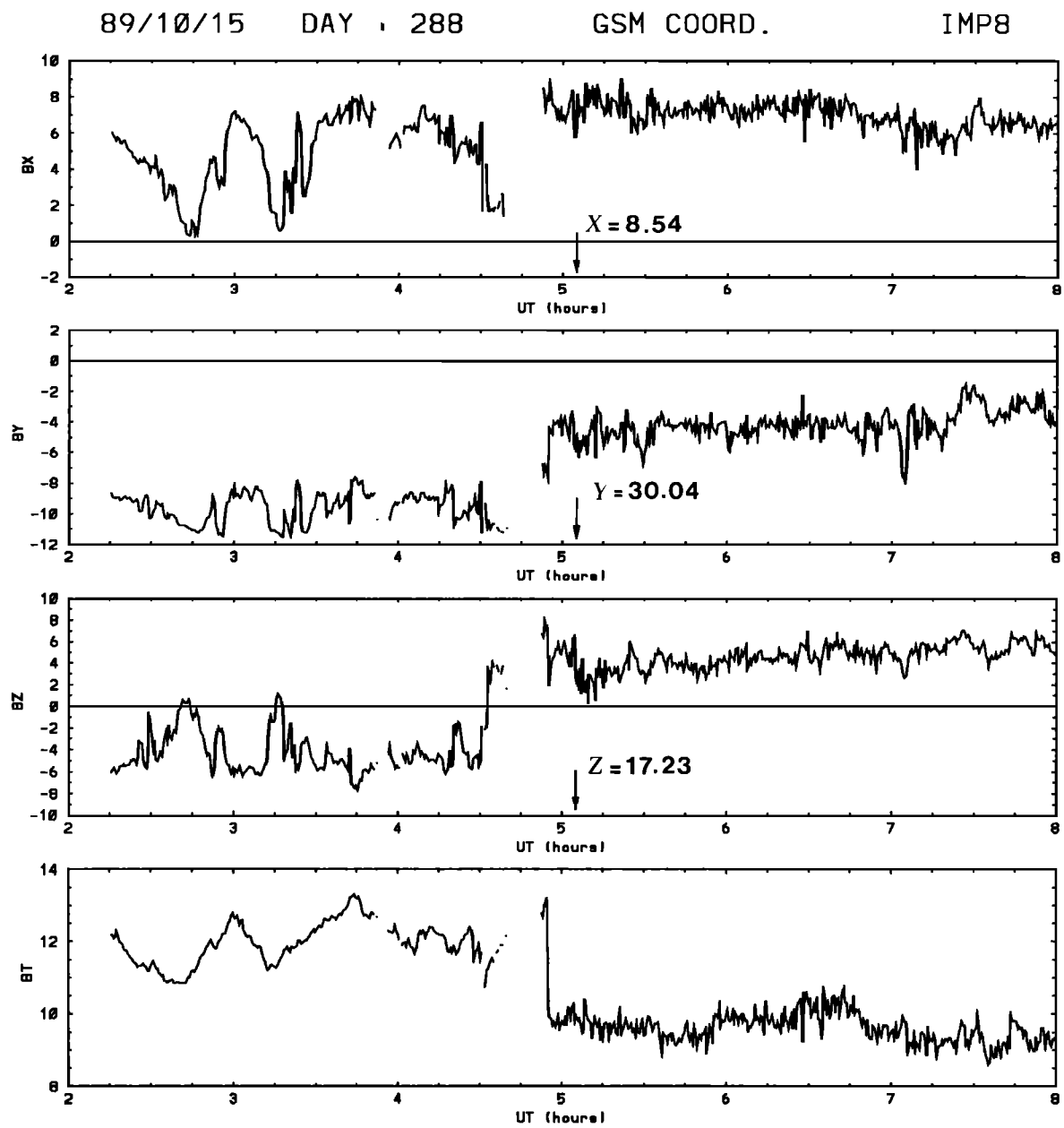

Fig. 4. IMP8 interplanetary magnetic field (IMF) measured on October 15, 1989, between 0200 and 0800 UT. The GSM coordinates of the satellite at the time shown by the arrows are given in units of Earth radii.

component occurred north of 70° invariant latitude and between 0300 UT and 0500 UT, i.e., in the ≈21-23 and ≈01-03 MLT sectors, respectively, for the Canopus and Greenland chains. These fluctuations did not exceed 50 nT, which indicates that the night sector was very quiet at the time of the B_Z reversal.

Radial Velocities

The raw data for the central beam 8 of the radars in Schefferville and Goose Bay during the period 0000 to 1200 UT are shown in Plate 1. Beam 8 is oriented east of geomagnetic north for both radars (see Figure 3). For both radars we have shown in the top panel the signal-to-noise ratio and in the bottom panel the Doppler (radial) velocity. Each of these quantities is color coded, as indicated to the right of each diagram. Echoes identified as ground scatter are coded in grey in the Doppler velocity frame. Positive velocities (blue) are directed toward the radar, while negative velocities (yellow to red) are directed away from the radar. The vertical axis of each plot is the distance from the radar, larger distances corresponding to higher latitudes, and the horizontal scale is UT time.

At Goose Bay, prior to about 0420 UT, there were very few echoes on beam 8 as well as on other beams. In contrast, echoes were present over several hundred kilometers on all Schefferville beams before 0420 UT, and dual-frequency operation extended the field of view of the radar. Despite this difference in echo occurrence the Doppler velocity along beam 8 had the same behavior at Goose Bay and Schefferville: radial velocities were small and mainly negative (corresponding to an eastward flow) at the beginning of the night and reverse at later UT times (corresponding to a westward flow). During this second period, both radars saw a region of large positive velocities which tended to move toward larger ranges, while

15 OCTOBER 1989

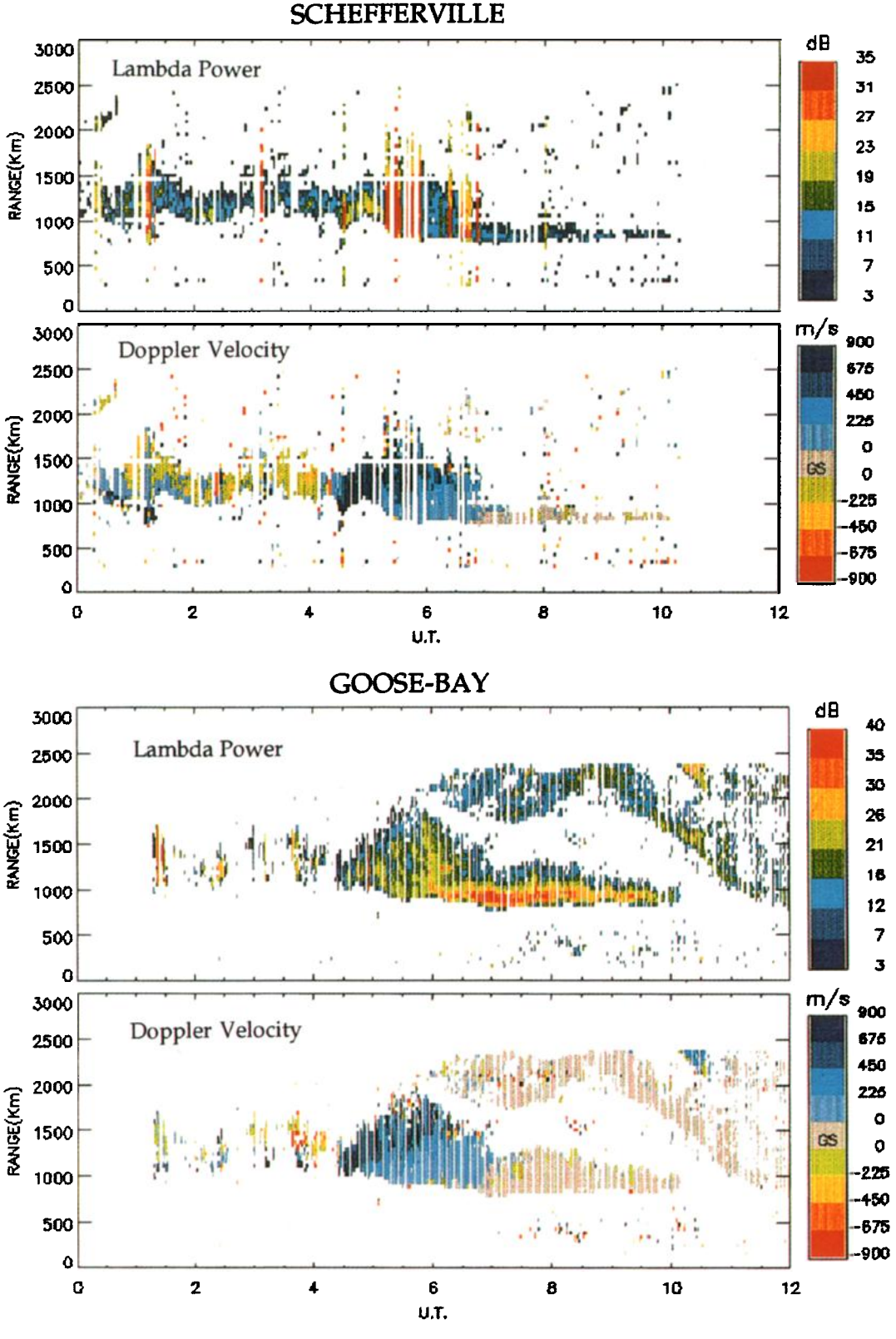

Plate 1. Time variations of the amplitude of the backscattered signal and the Doppler velocity for the central beam 8 of each radar. Negative velocities (green to red) are directed away from the radar and positive velocities (blue) are directed toward the radar. A reversal of the convection is observed around 0430 UT both at Schefferville and Goose Bay. Just after the reversal, very large velocities (between 650 and 900 m/s) are observed at all distances from the radar. Later, the region where these large velocities are observed moves progressively to larger ranges, while the velocity decreases at small ranges.

the velocities measured in the closest gates tended to decrease uniformly. The exact time of the velocity reversal is not easy to determine from Plate 1 due to data gaps and multiple reversals on beam 8. Our best estimate is that the reversal occurred between 0409 and 0422 UT at Schefferville and between 0413 and 0422 UT at Goose Bay.

Vector Velocity Maps

Figure 5 shows, for selected times between 0400 and 0630 UT, a set of eight convection maps obtained by the method described in the previous section. Each map was obtained by smoothing the data over 3 min, which corresponds to two successive azimuthal scans, thus allowing the dual-frequency operation of the Schefferville radar to extend the spatial coverage. At 0406 UT the common region of radar echoes was very small, and the convection was slow and eastward over the whole scatter zone between 0045 and 0200 MLT. Examination of the individual scans from Goose Bay and Schefferville indicates that this situation prevailed until about 0408-0410 UT, i.e., small radial velocities directed toward the radars on the western beams and away from the radars on the eastern beams.

Around 0410 UT a region of large radial velocities directed toward the radar appears on the eastern beams of the Schefferville radar, indicating that the flow is reversing to southwestward on the east side of the field of view. This region of southwestward velocities progressively extends to the western beams, at the rate of the Earth rotation. Although there are no echoes observed with the Goose Bay radar from 0410 UT to 0417 UT, the two radars show the same behavior afterward. A typical map from this time period is the one at 0427 UT (Figure 5*b*), where the flow reversal from eastward on the western side of the field of view to westward on the eastern side occurs around 0130 MLT.

The next two maps at 0430 and 0433 UT (Figures 5*c* and 5*d*) show that the eastward velocities have disappeared from the 0100 to 0130 MLT sector. This temporal change is also visible on individual maps of the radial velocities: indeed, while the Earth had rotated by 2° of longitude from 0426 to 0434 UT, the eastern region of large velocities directed toward the radar had progressed westward by about 8°. Another temporal change of this type (i.e., sudden westward penetration of the region of large westward velocities) is also seen on the radial velocity maps around 0443 UT, although it is not apparent on the 3-min average vector velocity maps.

In the time period between 0443 and 0700 UT the radial velocities from the two radars varied smoothly, without any sudden change. The last four maps of Figure 5 are representative of this period. They show the general trend of the plasma to drift southwestward in the early morning sector when B_z was positive and B_y negative. These maps also show the development of a region of small velocities, first observed in the southeastern part of the field of view at 0530 UT and then progressing northward in the radar common field of view. Finally, between about 0500 and 0630 UT, regions of radial velocities away from the radars (i.e., north to northeastward flows) are observed occasionally in the northern parts of the radar fields of view. These echoes are generally not observed simultaneously by the two radars.

Universal Time Variations

UT variations of the convection are not easily deduced from the comparison between successive maps, since the common field of view of the two radars drifts toward increasing MLTs as UT evolves. In order to obtain what can be called "true" UT variations, we have calculated latitudinal velocity profiles along magnetic meridians drifting from east to west through the field of view of the two radars, so that their MLT remains constant. Such profiles should remain stable in time if the convection pattern were time independent in a magnetospheric coordinate system. At the average UT of a single map, the velocity is determined along a particular magnetic meridian at a series of points separated by half a degree in latitude. At each of these points the velocity is obtained as a weighted average (by the inverse of the distance) of the closest data points (less than 0.5° in latitude and less than 1.0° in longitude). Results of this process are shown in Figure 6 along the 0315 MLT magnetic meridian. The straight lines issued from each point of the diagram are real velocities, the horizontal and vertical components representing, respectively, the geomagnetic east and north components of the velocity vector. At 0315 MLT the velocity latitudinal profile could be monitored from the dual radar system for about 2 hours.

The velocity was mostly westward over the latitudinal range 71°-77°, for the period from 0445 to 0700 UT, during which the 0315 MLT meridian drifted through the common field of view of the two radars. Figure 6 shows that the region of small velocities slowly progresses northward at a rate of about 2.0°-2.5° per hour. This poleward displacement was also seen on the radial velocities from the central beam (Plate 1). However, whereas spatial and temporal variations cannot be clearly separated from Plate 1, Figures 5 and 6 indicate that this displacement is both spatial and temporal. The same behavior (i.e., the slow northward displacement of the boundary between large and small velocities) was seen on all magnetic meridians that drifted through the radar field of view between 0445 and 0700 UT, i.e., for meridians from 0230 to 0400 MLT.

An estimation of the time constant of this slow reconfiguration can be obtained from Figure 7, where the amplitude of the velocity at 0315 MLT, averaged over the latitudinal range 72°-73.5°, is plotted versus UT. Figure 7 again shows the general trend of the velocity at low latitude to decrease with time. The least squares fit of an $\exp(-t/\tau)$ function to the data is given by the dashed line. It indicates a time constant of 1 hour.

DISCUSSION

Convection for Southward Interplanetary Magnetic Field (IMF)

Before 0410 UT, when the IMF was southward, the common region of echoes was very small and extended between about 73° and 76° invariant latitude and between 0030 and 0200 MLT. The position of the northern polar cap boundary deduced from particle data from the DMSP F8 and F9 satellites is plotted in Figure 8, and its latitude is given in Table 1. The DMSP data show that before the IMF reversal (i.e., for satellite passes before 0350 UT) the polar cap was very stable and located around 71.5° invariant latitude in the midnight sector and around 74.8° in the dawn sector. Therefore during this period the postmidnight radar observations correspond to a polar cap flow for $B_z < 0$ and $B_y < 0$. Empirical models [*Foster et al.*, 1986; *Heppner and Maynard*, 1987] give southward velocities of very small amplitude for this IMF orientation and local time sector. Our radar data partly agree with these models, in that the amplitude of the observed velocities is very small

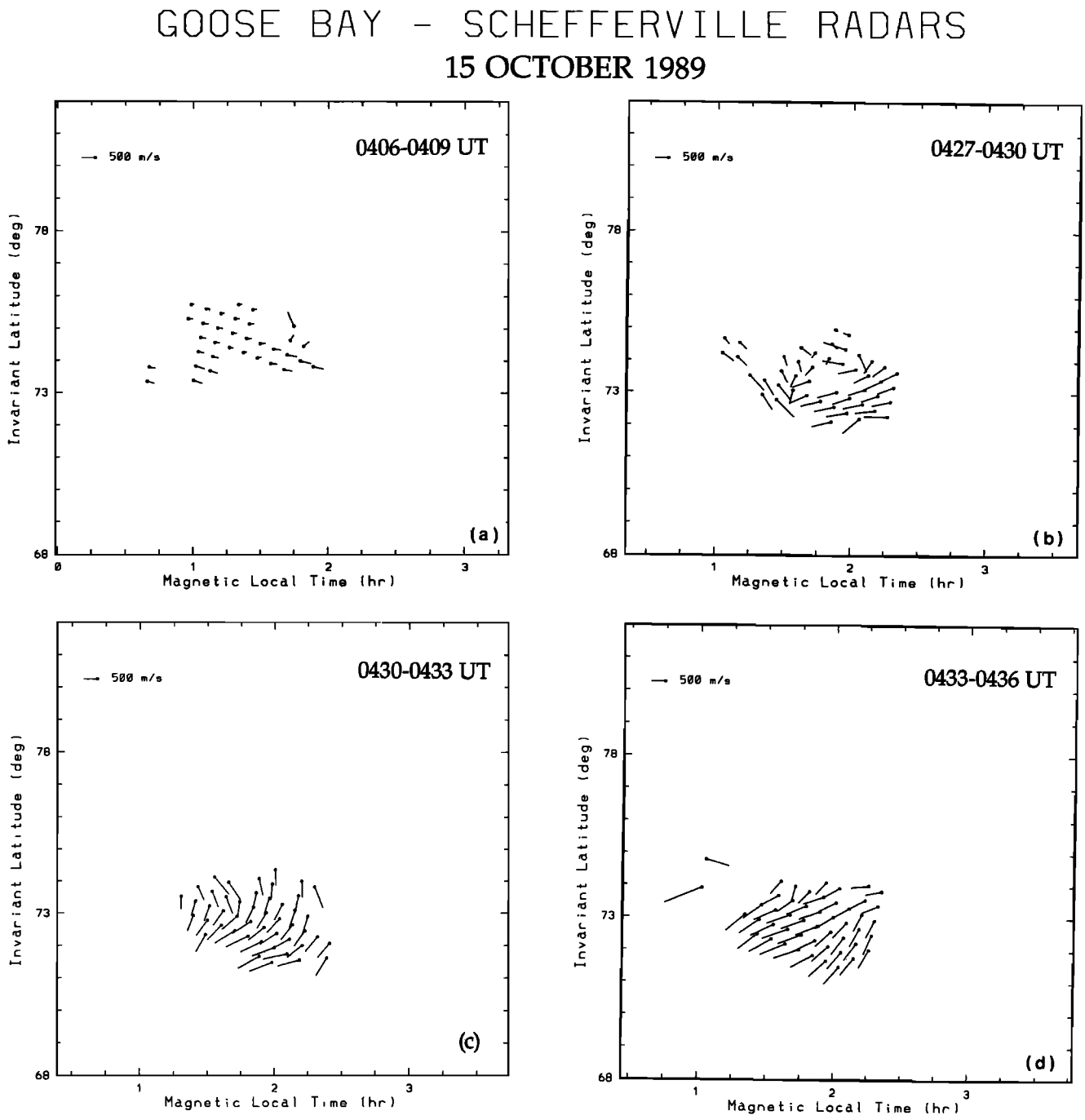

Fig. 5. Eight convection maps obtained by merging the radial velocity maps of Schefferville and Goose Bay on October 15, 1989, before and after the northward turning of the IMF at 0433 UT.

and the velocity has a southward component (Figure 5*a*). However, our data show an essentially eastward velocity, in opposition with both models. We have no explanation for this difference, except that it may be due to a day-to-day variability of the convection that is not described by statistical models.

Convection for Northward IMF

Although the two-cell convection pattern is well established both theoretically and experimentally for a southward IMF, there is much uncertainty on the structure of the plasma flow for northward IMF. *Reiff and Burch* [1985] suggested a four-cell convection pattern consisting of two lobe cells produced by merging on field lines tailward of the cusp and of two lower-latitude viscous cells. For $B_y < 0$ and in the morning sector, they predicted a complex structure of the flow with velocities reversing twice from eastward to westward and back to eastward, going from north to south. The westward flow, associated with the viscous cell, would be slow in this model. The early morning sector velocity data shown in Figure 5 do not support this model.

On the other hand, *Ogino et al.* [1985], in a numerical simulation of magnetospheric convection for B_z positive, found a much more complicated convection pattern that is schematically shown in Figure 9*a* for $B_y = 0$ and for the northern hemisphere. It consists of low-latitude viscous cells

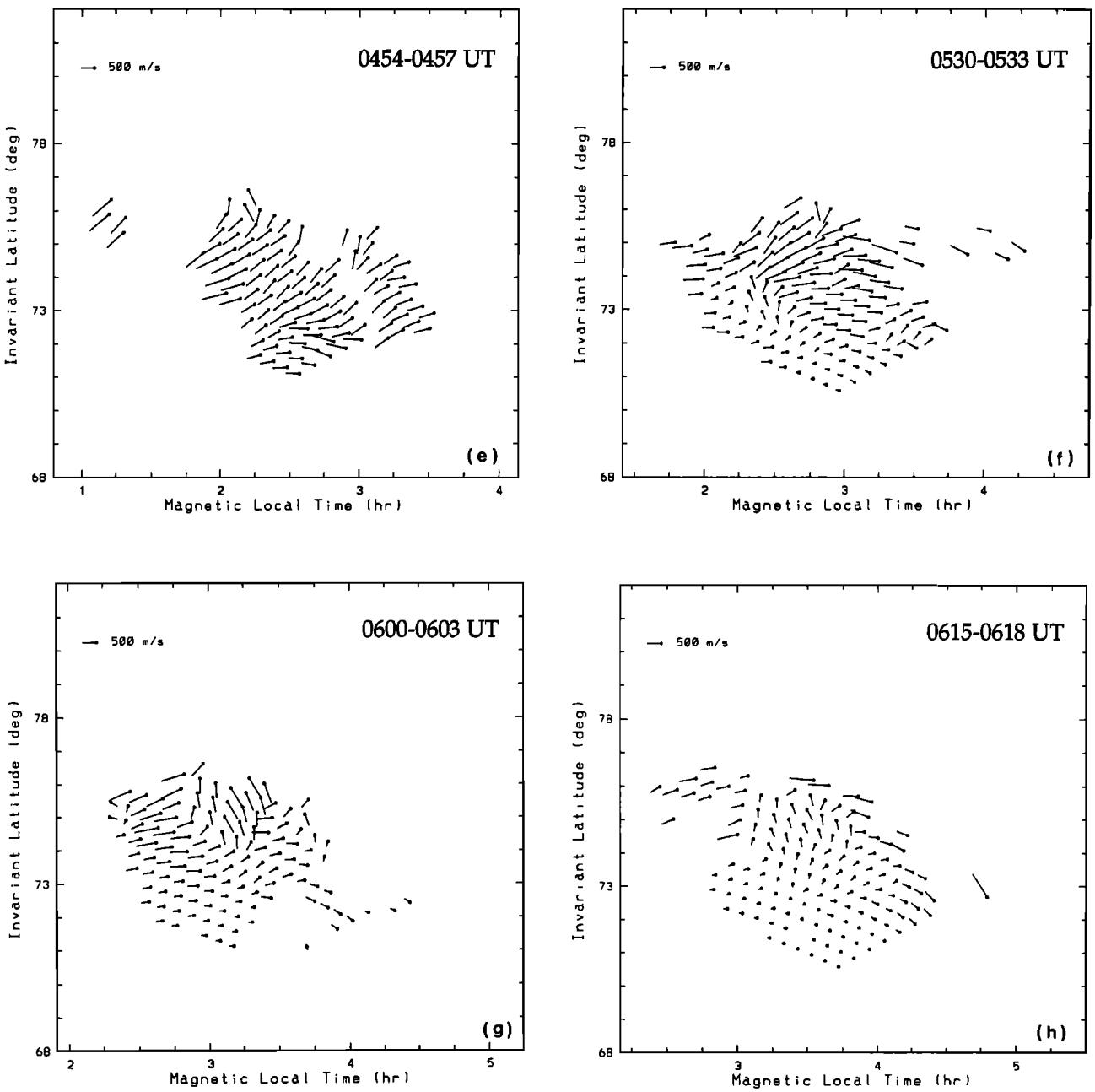

Fig. 5. (continued)

in the dayside (V_A) and nightside (V_L) on closed field lines, of dayside merging cells (M) on open field lines, and of tail reconnection cells (R) on both closed and open field lines. The pattern distorts considerably with B_y, and in the case of $B_y < 0$ (Figure 9*b*), the evening side tail reconnection cell moves toward dawn and eventually connects to the morning side merging cell.

In the early morning sector (0200-0500 MLT) and for the IMF conditions prevailing after 0433 UT on October 15, 1989, the *Ogino et al.* [1985] model of Figure 9*b* predicts that the flow is essentially southwestward over the latitude range probed by the Schefferville and Goose Bay radars, with possibly northeastward flows in the northern part of the fields of view. Furthermore, as indicated by the distance between equipotential contours in the original figures of *Ogino et al.* [1985], the southwestward flow associated with the convergence of the evening side R_1 and morning side R_2 tail reconnection cells would be rapid, whereas it would be slow in the morning side R_2 cell. All these characteristics are very consistent with the vector velocities shown in Figure 5 and, in particular, during periods when the IMF is steadily northward. Indeed, whereas the flow is predominantly southwestward after 0430 UT, large velocities of up to 700 m/s were observed everywhere in the field of view west of about 0300 MLT,

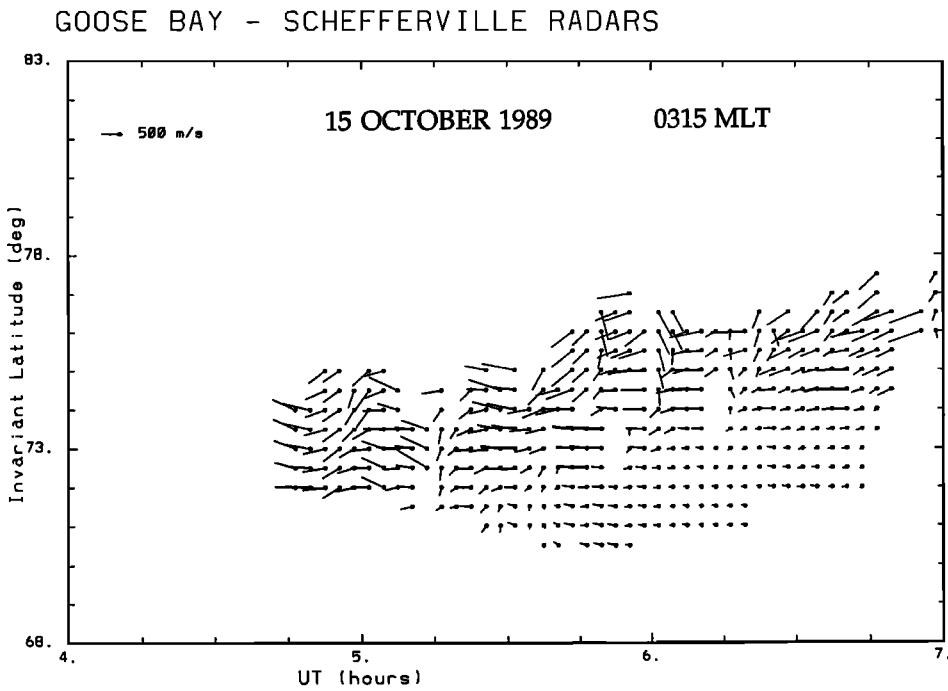

Fig. 6. "True" UT variations of latitudinal velocity profiles. The horizontal and vertical coordinates are UT and invariant latitude. Each vector represents the vector velocity calculated at the time and latitude of the initial dot for the fixed magnetic local time (MLT) of the figure (here 0315 MLT). Each point of this map drifts westward with UT through the fields of view of the radars.

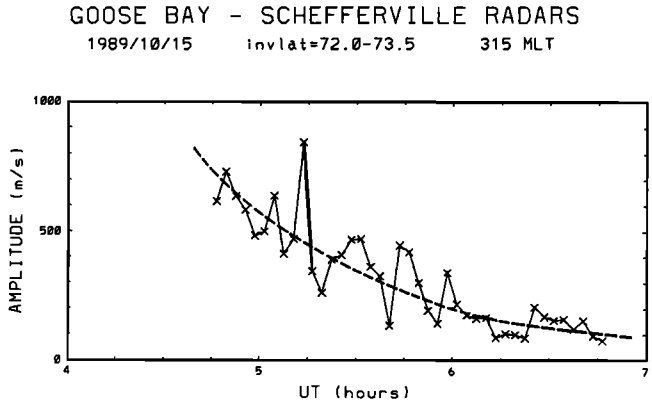

Fig. 7. Time variations of the amplitude of the velocity at 0315 MLT, averaged over 72°-73.5° invariant latitude. The dashed curve shows the least squares fit to the data.

whereas the flow was slow in the southern part of the field of view at later local times. In addition, the comparison of UT variations of the velocities along different magnetic meridians shows that the region of small velocities progresses northward as one proceeds toward dawn, as in the model. Finally, the maps of radial velocities indicate the presence of northeastward flow in the northern part of the radar fields of view, in regions where coincident data from the two radars are not available. This is also consistent with the modeled flow pattern of Figure 9.

In the southern hemisphere the convection pattern predicted by *Ogino et al.* [1985] for $B_z > 0$ and $B_y < 0$ is the mirror image, with respect to the noon-midnight meridian, of that of Figure 9*b*. In the early morning sector and around 75° invariant latitude it corresponds to small and irregular velocities. This is indeed what was observed by the Halley Bay radar which is conjugate to the Goose Bay and Schefferville radars (M. Pinnock, private communication, 1992).

We therefore believe that the model of *Ogino et al.* [1985] gives a correct representation of the convection pattern in the night sector for $B_z > 0$ and $B_y < 0$. This agrees with the observations of *Dudeney et al.* [1991], who studied the early morning convection patterns observed by the Halley Bay and Goose Bay radars for the same IMF orientation. In particular, they found westward convection velocities of 700-1000 m/s, i.e., of the same order of magnitude as those found here. More precisely, we associate the region of large velocities in the northern and western parts of the common radar field of view,

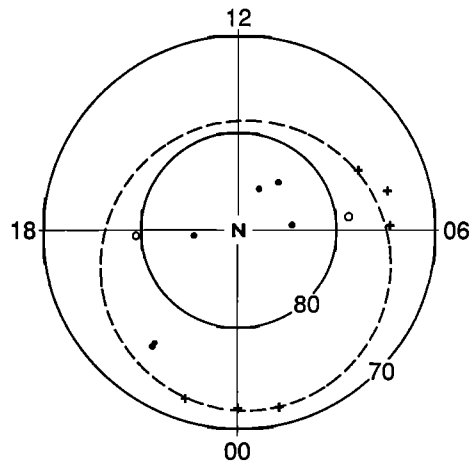

Fig. 8. Location of the polar cap boundary determined from DMSP particle data in an invariant latitude/MLT coordinate system. Data before the southward to northward IMF reversal (from 0025 to 0350 UT) are shown as crosses that align rather well along a circular polar cap plotted with a dashed line. Data after the IMF reversal are shown as open circles (at 0510 UT) and solid circles (from 0650 to 0851 UT). See also Table 1.

TABLE 1. Invariant Latitude of the Polar Cap Boundary Deduced From Particle Data From the DMSP F8 and F9 Satellites for Northern Hemisphere Passes

Hour, UT	0600-0700, MLT	2230-0100, MLT	2130-2140, MLT	1800-1900, MLT
0025	74.7	71.2		
0207	74.8	71.7		
0350		71.6		
0510	78.6			79.3
0650	84.3			85.3
0710			75.3	
0851			75.5	

The UT given is the approximate hour when the satellite is in the center of the polar cap along the pass. MLT, magnetic local time.

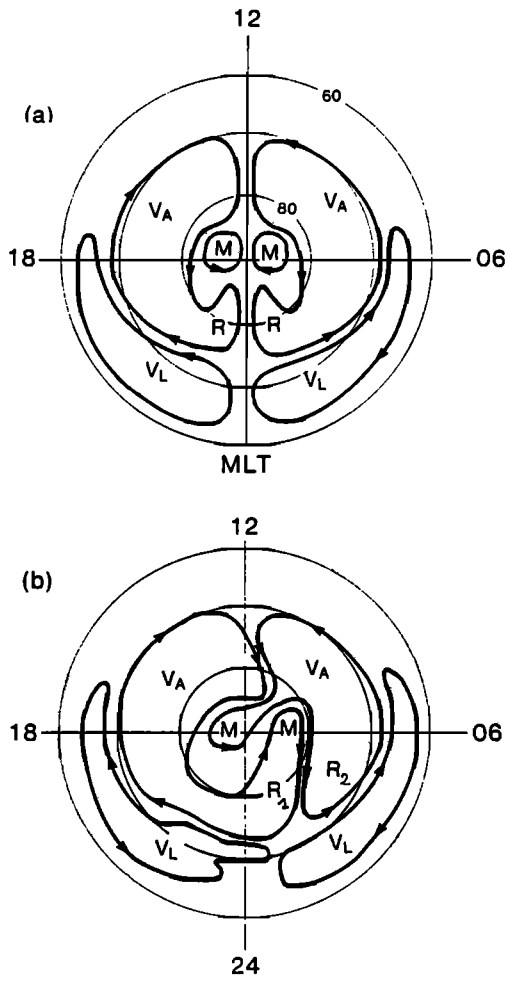

Fig. 9. Schematic diagram of the northern hemisphere high-latitude convection found by *Ogino et al.* [1985] for a northward IMF. (*a*) $B_y = 0$; (*b*) $B_y < 0$ and $|B_z/B_y|=1.7$. M, the high-latitude merging cells; V_A, the dayside viscous cells; R, the tail reconnection cells; and V_L, the low-latitude viscous cells. The figure is reproduced from *Dudeney et al.* [1991].

with the convergence between the tail reconnection cells R_1 and R_2 (located in the early morning sector for $B_y < 0$) and the region of small velocities in the southeastern part of the field of view with the morning-side tail reconnection cell R_2.

Time Variations of the Convection

Having identified the convection pattern for the period when the IMF was steadily northward, we can now address the question of time variation of the convection, in particular the way in which the nightside convection responded to the sudden IMF reversal at 0433 UT. Following *Lockwood et al.* [1989], we have estimated the time delay between the IMF B_z reversal impinging upon the IMP8 satellite at 0433 UT and the start of the response of the dayside ionosphere. This estimation relies on the assumption that the perturbation wave front was aligned with the IMF vector in the ecliptic plane and on assumed values of a number of parameters such as the distance from the Earth center of the subsolar bow shock X_b and magnetopause X_m, the solar wind velocity V_{sw}, the plasma velocity in the magnetosheath V_{sh}, and the transit time τ_{mi} of a single Alfvén wave from the magnetopause to the ionosphere. For the present calculation we have taken $X_m=11.7\ R_e$, $X_b=1.33\ X_m$, $V_{sw}=350$ km/s, $V_{sh}=V_{sw}/8$, and $\tau_{mi}=2$ min (see *Lockwood et al.* [1989] for the details of the calculation). These values are consistent with the particle data from IMP8, with the distances from the Earth and shapes of the magnetopause and bow shock found theoretically by *Spreiter and Stahara* [1980] and with the location of the bow shock inferred from the IMP8 magnetic field data of Figure 4. Using these values, we find that the dayside ionosphere should respond to the IMF reversal about 2 min after it was observed by the IMP8 satellite, i.e., around 0435 UT.

The nightside ionosphere on the other hand is believed to respond to IMF perturbations with a much larger time delay than the dayside ionosphere. For example, *Todd et al.* [1988], using data from the EISCAT radar showed that the delay between the time when an IMF perturbation impinges upon the subsolar magnetopause and the time when the ionosphere responds varies with MLT: the delay is 1-2 min at 1500 MLT and reaches 10-15 min at 0900 and 1800 MLT. *Dudeney et al.* [1991], in their study of an IMF B_y reversal for B_z north with the Goose Bay and Halley Bay radar data, found a time delay of about 25 min, roughly consistent with the transit time through a small polar cap of dimension ≈ 1500 km, characteristic of B_z north, at a velocity of 1 km/s.

It is thus very likely that the three rapid time variations of the convection observed by the radars at 0410, 0430, and 0443 UT, which bring the nightside convection pattern to a B_z north configuration, are not the result of the 0433 UT IMF reversal. In the absence of substorm activity in the nightside (see above) these time variations may be due to previous IMF perturbations (at least for the first two events), or to local effects. It is also possible that due to the long time it takes for nightside convection to reorganize after an IMF perturbation, the effects of new IMF perturbations will be superimposed on those from earlier perturbations, giving rise to complex temporal variations.

Evidence for the slow reconfiguration of the nightside convection was given in the previous section and, in particular, in Figures 6 and 7. *Knipp et al.* [1991], using ground magnetometer and radar data together with the assimilative mapping of ionospheric electrodynamics (AMIE) technique described by *Richmond and Kamide* [1988], also found a slow reconfiguration of the nightside convection which lasted more than 1 hour, after a northward turning of the IMF. Their estimation is consistent with the time constant of 1 hour derived from Figure 7. However, whereas we observe a

general poleward displacement of the convection pattern, they find a slow decay of the convection. The difference between their observations and our observations for the same IMF behavior may be due to the sparse nightside data coverage that Knipp et al. used as input to the AMIE inversion technique.

It is interesting to note here that although the observed postmidnight convection pattern agrees with the *Ogino et al.* [1985] model, the reconfiguration time constant of roughly 1 hour deduced from our data is larger than the time necessary for the Ogino et al. pattern to reach a quasi-steady state, which is 32 min. Neutral winds may well play an important role in slowing down the ionospheric process. Indeed, *Deng et al.* [1991] have shown that inertial effects due to the atmospheric dynamo can maintain the plasma convection for several hours after a magnetic storm. Such inertial effects are not included in the Ogino et al. model, which completely lacks the ionospheric part of the circuit.

Let us now consider the various manifestations of the slow reconfiguration of the polar ionosphere in response to the B_z northward turning and, in particular, the MLT dependency of its time constant. First, a northward displacement of the polar cap boundary is observed from the DMSP particle data. Figure 8 and Table 1 show that after a long period of stability corresponding to $B_z < 0$, the polar cap boundary in the dawn sector moved from 74.8° invariant latitude for $B_z < 0$ to 78.6° at 0510 UT and to 84.3° at 0650 UT, after the B_z reversal. The northward displacement of the boundary at dawn thus occurred at a rate of about 3.4°/h, similar to the rate observed at dusk. In the 2100 MLT sector the polar cap contraction occurred at a much slower rate. With the assumption of a circular polar cap whose center is shifted toward dawn (in agreement with DMSP data reported by *Holzworth and Meng* [1984]) and 4° antisunward before the B_z reversal, this rate does not exceed 3° in more than 3 hours.

Secondly, the boundary between large and small velocities observed in the radar data at 0315 MLT moves northward at a rate of about 2.0°-2.5°/h between 0530 and 0630 UT, in response to the B_z reversal (Figure 6). Table 2 gives the time constant of the slow decrease of the velocity in the 72°-73.5° invariant latitude range for magnetic meridians separated by 15 min between 0230 and 0330 MLT. These time constants have been deduced from plots similar to Figure 7. Table 2 shows that the time constant consistently decreases with MLT. In other words the convection pattern in the postmidnight sector reconfigurates more slowly as one proceeds toward midnight.

If we assume that the polar cap boundary and the boundary between large and small velocities move together with the same velocity and if we further assume that larger velocities of the boundary correspond to smaller reconfiguration time constants, then the previous data are consistent with a movement of the boundaries with a velocity that depends upon MLT. This velocity is larger at dawn and dusk than at 0315 MLT (i.e., rates of 3.4°/h and 2.0°-2.5°/h respectively) and larger at 0315 than at 2100 MLT where it does not exceed 1°/h. In addition, it decreases as one proceeds toward midnight in the postmidnight sector between 0230 and 0330 MLT. Therefore it appears that the polar cap contracts more rapidly in the dayside than in the nightside and more rapidly in the postmidnight sector than in the premidnight one.

TABLE 2. Time Constant of the Velocity Decrease at Various MLTs

MLT, hour	τ, min
0230	82
0245	72
0300	75
0315	60
0330	59

Velocities are averaged in the latitudinal range 72°-73.5°.

Because open magnetic flux stops entering the polar cap through the dayside after an IMF B_z northward turning, it seems natural that the contraction of the polar cap occurs over shorter time scales in the dayside than in the nightside. Indeed, *Meng and Makita* [1986], in a case study of the polar cap size from DMSP particle data, found a similar asymmetry between day and night. On the contrary, the premidnight/postmidnight asymmetry cannot be easily understood in terms of dayside reconnection processes. It is possible that an additional mechanism operates in the night sector, which removes open magnetic flux from the polar cap preferentially in the postmidnight sector. A good candidate would be the nightside exit zone predicted by the *Ogino et al.* [1985] model between the R_1 and the R_2 tail reconnection cells, which is located in the postmidnight sector for $B_y<0$ (Figure 9). Further simulation of the time variations of the convection after a B_z northward turning would be necessary to check if the Ogino et al. model can predict such a local time dependency of the reconfiguration process.

CONCLUSION

The unique capability of HF radars to provide plasma Doppler velocities of the plasma in the F region over extended fields of view with a time resolution of 1-2 min has been used to separate the spatial and temporal variations of the high-latitude convection pattern after an IMF southward to northward reversal. Radial velocities from the French Schefferville (Quebec) and American Goose Bay (Labrador) radars, whose fields of view overlap over Greenland and northeastern Canada, have been merged for the first time to provide instantaneous maps of the plasma flow without any additional assumptions on the structure of the flow. From these maps the "true" UT time variations of the flow along selected magnetic meridians have been followed during several hours as they rotate through the common radar field of view.

We have studied in detail the convection pattern in the early morning sector on October 15, 1989, when the IMF B_z component reversed from southward to northward, while the B_y component remained negative. The exact time at which the nightside convection started to respond to the IMF B_z reversal could not be precisely determined from our data set. Temporal changes occurring close to and even anticipating the B_z reversal are thought to be associated with the delayed and superposed responses from previous IMF perturbations or to local effects.

The observed early morning convection features for steady $B_z > 0$ and $B_y < 0$, with westward and southwestward velocities in the 71°-77° invariant latitude range, are consistent with the numerical simulations of *Ogino et al.* [1985]. In the context of this model our observations correspond to the flow in the two tail reconnection cells, both located in the early morning sector for $B_y < 0$. After a southward to northward IMF B_z turning, the convection pattern in the early morning sector is observed to reconfigure slowly. During this slow

reconfiguration the convection fades away in the southern part of the radar common field of view, and the region of intense convection moves poleward. The time constant of this slow reconfiguration is one hour at 0315 MLT and increases toward midnight. It is larger than that predicted by the MHD simulation of *Ogino et al.* [1985] for which a quasi-steady state magnetospheric configuration is obtained after 32 min.

These HF radar data, combined with particle data recorded along successive passes of the DMSP satellites, provided information on the MLT variations of the polar cap contraction velocity after the southward to northward turning of the IMF. They showed, in particular, that the polar cap contracts more rapidly in the daytime than in the nightime and more rapidly in the postmidnight sector than in the premidnight one. It was suggested that this latter asymmetry could be the manifestation of a region, located in the 0300 MLT sector for $B_y < 0$, from where open magnetic flux exits the polar cap.

The data presented in this paper illustrate the unique opportunity given by HF coherent bistatic radar systems for separating spatial and temporal variations in the flow pattern, therefore contributing significantly to the understanding of ionospheric response to changes in the interplanetary magnetic field. However, the effective field of view of such systems is limited to a region smaller than a single convection cell. The SuperDARN project, consisting of eight HF radars distributed at high latitudes in the northern hemisphere from Finland to Alaska has recently been proposed to overcome this limitation. This radar project, which is now under construction, will extend the instantaneous coverage to nearly 14 hours of magnetic local time and thus provide instantaneous maps of large parts of the convection cells.

Acknowledgments. We thank Mike Pinnock for enlightening discussions and C. Margaret-Mary for initiating the work of separating spatial and temporal variations in the HF radar data. We also thank P. Newell, R. Lepping, E. Friis-Christensen, and T. Hugues for providing us, respectively, with the DMSP, IMF, Greenland, and Canopus ground magnetometer data. The operation of the SHERPA radar in Schefferville is supported by the Institut National des Sciences de l'Univers (INSU). This study has been also partly funded by the Direction des Recherches et Etudes Techniques (DRET). We wish particularly to thank Yves Ruin for setting the radar and keeping it operating and Oksana Choulik and staff at the McGill Subarctic Research Station for daily operation of the radar. The radar at Goose Bay is supported by the National Science Foundation, Division of Atmospheric Sciences, under NSF grant ATM-9003860 and by the National Aeronautics and Space Administration (NASA) under NASA grant NAG5-1099.

The editor thanks E. Nielsen and S. Buchert for their assistance in evaluating this paper.

REFERENCES

Baker, K. B., and S. Wing, A new magnetic coordinate system for conjugate studies at high latitudes, *J. Geophys. Res., 94,* 9139, 1989.

Baker, K. B., R. A. Greenwald, A. D. M. Walker, P. F. Bythrow, L. J. Zanetti, T. A. Potemra, D. A. Hardy, F. J. Rich, and C. L. Rino, A case study of plasma processes in the dayside cleft, *J. Geophys. Res., 91,* 3130, 1986.

Deng, W., T. L. Killeen, A. G. Burns, and R. G. Roble, The flywheel effect: Ionospheric currents after a geomagnetic storm, *Geophys. Res. Lett., 18,* 1845, 1991.

Dudeney, J. R., A. S. Rodger, M. Pinnock, J. M. Ruohoniemi, K. B. Baker, and R. A. Greenwald, Studies of conjugate plasma convection in the vicinity of the Harang discontinuity, *J. Atmos. Terr. Phys., 53,* 249, 1991.

Foster, J. C., J. M. Holt, R. G. Musgrove, and D. S. Evans, Solar wind dependencies of high-latitude convection and precipitation, in *Solar Wind-Magnetosphere Coupling,* edited by Y. Kamide and J. A. Slavin, p. 477, Terra Scientific, Tokyo, 1986.

Freeman, M. P., J. M. Ruohoniemi, and R. A. Greenwald, The determination of time-stationary two-dimensional convection patterns with single-station radars, *J. Geophys. Res., 96,* 15,735, 1991.

Greenwald, R. A., K. B. Baker, and J. P. Villain, Initial studies of small-scale F region irregularities at very high latitudes, *Radio Sci., 18,* 1122, 1983.

Greenwald, R. A., K. B. Baker, R. A. Hutchins, and C. Hanuise, An HF phased array radar for studying small-scale structure in the high latitude ionosphere, *Radio Sci., 20,* 63, 1985.

Greenwald, R. A., K. B. Baker, J. M. Ruohoniemi, J. R. Dudeney, M. Pinnock, N. Mattin, J. M. Leonard, and R. P. Lepping, Simultaneous conjugate observations of dynamic variations in high latitude dayside convection due to changes in IMF B_y, *J. Geophys. Res., 95,* 8057, 1990.

Hanuise, C., J.-P. Villain, and M. Crochet, Spectral studies of F-region irregularities in the auroral zone, *Geophys. Res. Lett., 8,* 1083, 1981.

Hanuise, C., R. A. Greenwald, and K. B. Baker, Drift motions of very high latitude F-region irregularities: Azimuthal Doppler analysis, *J. Geophys. Res., 90,* 9717, 1985.

Heppner, J. P., and N. C. Maynard, Empirical high-latitude electric field models, *J. Geophys. Res., 92,* 4467, 1987.

Holzworth, R. H., and C.-I. Meng, Auroral boundary variations and the interplanetary magnetic field, *Planet. Space Sci., 32,* 25, 1984.

Keskinen, M. J., and S. L. Ossakow, Theories of high-latitude ionospheric irregularities: A review, *Radio Sci., 18,* 1077, 1983.

Knipp, D. J., A. D. Richmond, B. Emery, N. U. Crooker, O. de la Beaujardière, D. Evans, and H. Kroehl, Ionospheric convection response to changing IMF direction, *Geophys. Res. Lett., 18,* 721, 1991.

Lockwood, M., P. E. Sandholt, S. W. H. Cowley, and T. Oguti, Interplanetary magnetic field control of dayside auroral activity and the transfer of momentum across dayside magnetopause, *Planet. Space Sci., 37,* 1347, 1989.

Meng, C. I., and K. Makita, Dynamic variations of the polar cap, in *Solar Wind-Magnetosphere Coupling,* edited by Y. Kamide and J. A. Slavin, p. 477, Terra Scientific, Tokyo, 1986.

Ogino, T., R. J. Walker, M. Ashour-Abdalla, and J. M. Dawson, An MHD simulation of B_y-dependent magnetospheric convection and field-aligned currents during northward IMF, *J. Geophys. Res., 90,* 10 835, 1985.

Reiff, P. H., and J. L. Burch, IMF B_y-dependent plasma flow and Birkeland currents in the dayside magnetosphere, 2, A global model for northward and southward IMF, *J. Geophys. Res., 90,* 1595, 1985.

Richmond, A. D., and Y. Kamide, Mapping electrodynamic features of the high-latitude ionosphere from localized observations, 1, Technique, *J. Geophys. Res., 93,* 5741, 1988.

Ruohoniemi, J. M., R. A. Greenwald, K. B. Baker, J. P. Villain, and M. A. McCready, Drift motions of small-scale irregularities in the high-latitude F region: An experimental comparison with plasma drift motions, *J. Geophys. Res., 92,* 4553, 1987.

Ruohoniemi, J. M., R. A. Greenwald, J.-P. Villain, K. B. Baker, P. T. Newell, and C.-I. Meng, Coherent HF radar backscatter from small-scale irregularities in the dusk sector of the subauroral ionosphere, *J. Geophys. Res., 93,* 12,871, 1988.

Ruohoniemi, J. M., R. A. Greenwald, K. B. Baker, J. P. Villain, C. Hanuise, and J. Kelly, Mapping high-latitude plasma convection with coherent HF radars, *J. Geophys. Res., 94,* 13,463, 1989.

Shen, C.-S., and E. Nielsen, The spatial component of ionospheric electron flow derived from two-dimensional drift measurements, *J. Geophys. Res., 92,* 305,1987.

Spreiter, J. R., and S. S. Stahara, A new predictive model for determining solar wind-terrestrial planets interactions, *J. Geophys. Res., 85,* 6769, 1980.

Todd, H., S. W. H. Cowley, M. Lockwood, D. M. Willis, and H. Lühr, Response time of the high-latitude dayside ionosphere to sudden changes in the north-south component of the IMF, *Planet. Space Sci., 36,* 1415, 1988.

Villain, J.-P., R. A. Greenwald, and J. F. Vickrey, HF ray-tracing at high latitudes using measured meridional electron density distributions, *Radio Sci., 19*, 359, 1984.

Villain, J.-P., G. Caudal, and C. Hanuise, A SAFARI-EISCAT comparison between the velocity of F region small-scale irregularities and the ion drift, *J. Geophys. Res., 90*, 8433, 1985.

Villain, J.-P., R. A. Greenwald, K. B. Baker, and J. M. Ruohoniemi, HF radar observations of E region plasma irregularities produced by oblique electron streaming, *J. Geophys. Res., 92*, 12,327, 1987.

K. B. Baker, R. A. Greenwald, and J. M. Ruohoniemi, Applied Physics Laboratory, Johns Hopkins Road, Laurel, MD 20707.

J.-C. Cerisier and C. Senior, Centre de Recherches en Physique de l'Environnement / CNRS, 4 Avenue de Neptune, 94107 Saint-Maur-des-Fossés, France.

C. Hanuise, Laboratoire de Sondages Electromagnétiques de l'Environnement Terrestre / CNRS, Université de Toulon et du Var, BP 132, 83957 La Garde Cedex, France.

J.-P. Villain, Laboratoire de Physique et Chimie de l'Environnement / CNRS, 3A Avenue de la Recherche Scientifique, 45045 Orléans, France.

(Received November 23, 1992;
revised March 2, 1993;
accepted March 23, 1993.)